Real-time Detection of EEG Electrode Displacement for Brain-Computer Interface Applications

Giulia Cisotto and Silvano Pupolin
Department of Information Engineering
University of Padua
{giulia.cisotto & silvano.pupolin}@dei.unipd.it

***Abstract* – Electroencephalography (EEG) has a relatively old history since Hans Berger in 1929 recorded the human brain activity for the very first time. Since then, a number of experiments had led to a strengthened employment of this technology both in the clinical practice and in the most advanced research platforms. Although amazing developments have already been achieved, no gold standards are available for the processing of EEG signals. However, EEG signal processing used in several applications of Brain-Computer Interface (BCI) has already promised unbelievable progresses. In the context of a specific BCI application, this paper deals with a particular kind of artifact due to electrode-pops that can degrade the EEG recordings and, consequently, make BCI give wrong outputs to patients operating it for their benefit in recovery or in daily life.**

Keywords – EEG, BCI, electrode-pop artifact, online algorithm.

I. INTRODUCTION

Electroencephalography (EEG) [1] has a relatively old history and nowadays all Hospitals, clinical Institutes and even Universities have an EEG system to perform daily clinical assessments of several kinds of patients or to study the cerebral activity of healthy and impaired people in a relaxation status or during a task execution. Although its widespread availability, no gold standards for the analysis of the EEG traces are recognized all over the world. Instead most clinicians analyze by-eye only the cerebral activity of their patients being satisfied to observe macroscopic changes like epileptic seizures or alternating phases of more or less reactive awareness represented by larger or smaller oscillations in the frequency band around 10 Hz, the so-called α band. However research has already shown, in many years of study, that an amount of information is hidden in this complex combination of waves that EEG is.

One of the most amazing fields of EEG employment is the Brain-Computer Interface (BCI): after a training period, a subject can learn to operate a computer to communicate in an alternative way with the external world or to move again by controlling a wheelchair or a robotic arm [2].

This paper deals with a specific kind of EEG artifact that can arise from the displacement of an electrode during recordings. This event can cause the subject to fail in operating a BCI – at least for a limited period of time - because of the artefactual analysis of the correspondent EEG signal affected by the huge abnormal peak and oscillations following the displacement.

II. ELECTRODE-POP ARTIFACT IN EEG RECORDINGS

EEG recordings at the scalp of a subject are a combination of useful signal and disturbance. To be precise, the former is constituted by the neural response of the subject to an experimental task or, simply, it carries the information about the status of the individual, and the latter is the sum of all the other components of the EEG traces. As mentioned before, there can be several causes of disturbance but, generally, they are classified as follows:

a) external interferences. The main element of this set is the power line noise that usually corrupts the EEG recordings. For this reason, a notch filter around 50 Hz or 60 Hz is implemented to remove this considerable interference during EEG evaluations or experimental sessions.

b) *physiological interferences*. They can be further divided into two subclasses: muscular and neural noises. Eye-blinks, eye-gaze changes, chewing, gnashing, swallowing and head slight movements are muscles activations that can compromise the whole recordings. Skin sweat can be also a relevant phenomenon to cope with sometimes. Finally, distractions, habituation and other collateral cognitive phenomena can elicitate neural populations of different cortical regions to spike and, at the scalp level, to show interfering waveforms. The latter are considered disturbance and are usually removed on the basis of their spatial and/or frequency occurrence.

Then artifacts can occur either accidentally or along the whole recording. For instance, artefactual activity due to mains is usually present along the entire registration while muscular contraction is in the most cases a very short phenomenon that can seriously corrupt a relatively short-lasting recording segment. One of the most impacting causes of artifact is the so-called *electrode-pop*: although quite rare, this kind of noise can be completely superimposed over the low amplitude useful signal and make the identification procedure of the EEG characteristics almost impossible for a long time (tens of seconds). A typical example of its shape is captured by Fig.1 where the usual abrupt negative fall, overshoot and slow-oscillating return to baseline values are clearly visible.

It can be easily expected that such an artefactual activity compromises any kind of automatic features identification.

Cautions in order to avoid this kind of artifacts can be taken during the recording preparation: clinical technicians are trained to pay attention on this type of occurrence. Nevertheless electrode-pops can sometimes happen anyway. A hardware solution to cancel out this artifact has been proposed in [3] although without any quantification of its performance.

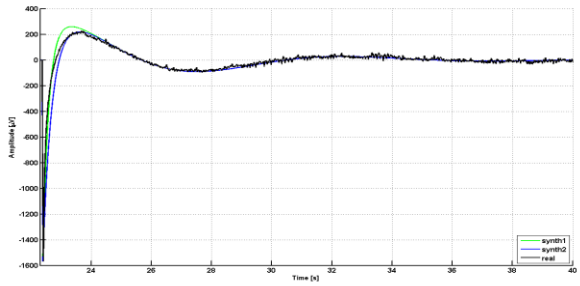

Fig. 1 Signal with electrode-pop artifact. A detail.

Several software solutions to remove artifacts have appeared in the past years [4-9]. The main objective of these solutions was to obtain a clear EEG signal for clinician eye-analysis. Our objective is somewhat different because we want to extract from EEG some real-time features to be used as feedback in BCI applications.

Hereafter a new real-time signal processing algorithm is presented with the aim to identify and remove this electrode-pop artifact before to estimate the EEG features required to assess the patient's status or to operate an EEG-based external device in a BCI fashion scheme.

III. Real-time algorithm for electrode-pop artifact

We consider the BCI treatment for motor recovery of the upper limb in stroke survivors described in [10], where the signal processing unit runs the world-spread software BCI2000 [11] which does not care about the electrode-pop artifact. Unfortunately, some recorded sessions of the whole BCI treatment were affected by this electrode displacement. We remark that feedback to the patient should be given in real-time based on *Movement-Related Desynchronization* (*MRD*) [12] of EEG signal. The presence of artifact prevents us to properly detect the MRD for several seconds. A new algorithm was designed and implemented with the goal to be performed in real-time during the BCI experiment and to reduce the time where MRD cannot be detected as short as we can. This algorithm has to be little time-consuming to allow the BCI system to process the remaining on-line analysis and provide the robotic feedback to the subject performing the experiment before he/she starts to execute the movement task.

In order to quantify the algorithm performance, the signal-to-disturbance-ratio (SDR) has to be computed. This would be possible only if a version of the same signal with and without the disturbance is available. To this purpose, a synthetic electrode-pop artifact was constructed and then added to a real EEG signal where no disturbance affected the trace. Then, the SDR is computed.

The artifact shown in Fig.1 is typical for each class of EEG amplifiers. Indeed, the first part, spanning few tens of milliseconds, is directly related to the amplifier bandwidth, while the second part, which shows a damped oscillation, is due to the AC coupling of the electrode to the amplifier.

Two different shapes of synthetic artifacts, similar to the real one, have been chosen for the following analysis and are displayed in Fig. 2 with a detail in Fig. 3.

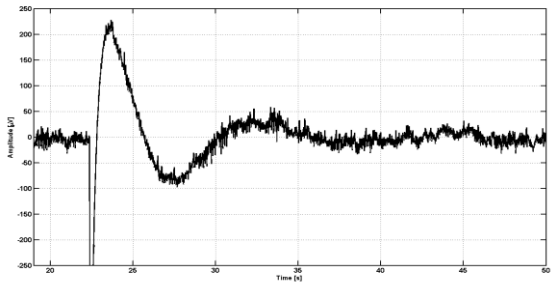

Fig. 2 Raw signal (black) and two different examples of synthetic artifacts.

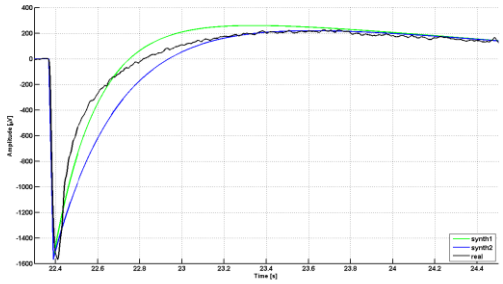

Fig. 3 Detail of Fig.2.

We remark that the artifact has an amplitude two order of magnitude larger than the EEG signal. To cancel the effects of this large disturbance only a nonlinear procedure works. We considered two different algorithms: i) estimate the main pulse and canceling it or ii) detect the time instant when the main pulse starts and set the signal to zero until it returns to zero. The first solution would be more precise but it would require a bunch of computations and an accurate model of the artifact to estimate the main pulse with enough precision. On the contrary the second algorithm has two main steps: 1) compute the first derivative of EEG signal as the difference between each sample and the previous one, and 2) determines where the absolute value of the derivative is higher than a threshold for N consecutive samples. Indeed, the electrode-pop could be represented as the impulse response of the amplifier filter. The rise-time t_r is related to the 3dB bandwidth B_s of the filter by the approximated relationship $t_r \approx 1/(3B_s)$. Hence, the rise-time span over $N=F_c t_r$ consecutive samples, where F_c is the sampling rate of the EEG. As an example, if F_c is set to 512 Hz and B_s is 20 Hz, N is about 8. The beginning of the artefact is given by the first sample where the derivative is higher than the threshold and the end by the sample where the EEG signal returns to zero. Then, the EEG samples between these points are replaced by zeros and discarded from the MRD detection. The zeros substitution between the two zero-crossing points is justified by the concern that filtering can give rise to transient signals due to possible abrupt signal discontinuities at the artefactual interval edges. During the interval of time where artifact is removed no feedback is intended to be provided to the subject but the system is thought to be waiting for new reliable values. An example of application of this method is reported in Fig.4 where the sum of an original artifact-free signal (recorded from the FZ site on the scalp) and a synthetic electrode-pop (black curve) is displayed along with its first

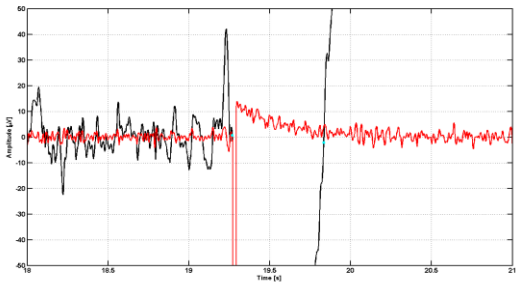

Fig. 4 Artifact-addicted EEG signal (black), its derivative (red) and the artefactual interval edges (cyan dots).

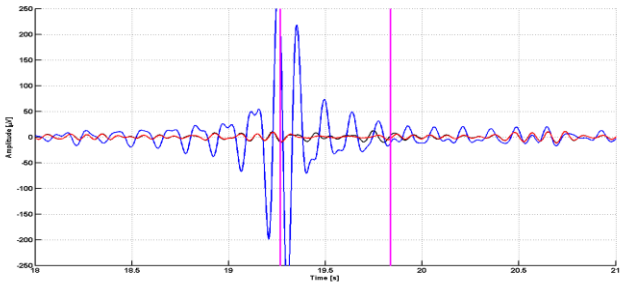

Fig. 5. The original raw signal filtered in the (7,14) Hz band (black curve), the filter output after the application of the proposed algorithm (red curve), the filter output without any artifact detection algorithm (blue curve) and the artefactual interval (magenta vertical lines).

derivative (red curve), and the two time instants labeled as the edges of the artefactual period are highlighted with cyan dots.

After these two first steps, the standard BCI2000 or another procedure involving a high-pass filtering above 1 Hz can be run as usual. The latter leads to the cancellation of the large remaining slow oscillation following the huge negative abrupt fall just removed, bringing back the signal to fluctuate around reliable values again. The zeros-fulfilled artefactual interval is filtered too and small oscillations arise at the filter output: however this does not represent an issue since this period of time is completely discarded from the following analysis. The difference between the (7,14) Hz band filter output with a previous step of artifact detection and removal and the same output without that preliminary operation is plotted in Fig.5. The (7,14) Hz band filtered version of the original raw signal without the synthetic artifact is also reported in both figures as a comparison. Moreover, two magenta vertical lines define the artefactual interval that is discarded from the following analysis.

Fig.5 shows that ideally-filtering a signal with an electrode-pop artifact causes an evident non-causal response that compromises the following analysis. Moreover, a real case filter would also introduce a significant delay that must be limited to make the BCI feedback reliable. On the contrary, filtering the EEG signal with the artifact removed does not cause any significant disturbance. The latter considerations are confirmed by the analysis of the performance presented later on.

Let us denote the original EEG signal filtered in the (7,14) Hz band as x while the filter output without the algorithm application as y_1 and the same quantity with the artifact previously detected and removed as y_2. Then e_1 and e_2 are defined as the following differences:

$$e_1 = y_1 - x \quad \text{and} \quad e_2 = y_2 - x$$

represent the errors between the filter output and the original artifact-free signal.

In order to quantify the algorithm performance, the error energy M_e, the signal energy M_x and the SDR (computed as the ratio between M_x and M_e) at the filter output was computed over 256 samples-wide time windows. Such a window width was chosen to be the same as that used by the BCI2000 software currently operating in the online procedure during the BCI experiment.

Then the new algorithm was employed in an offline analysis to assess its effectiveness. The goal of this analysis was to detect the presence of MRD during the BCI experiment described in [10].

III. Results

Let s be the original raw EEG signal and a the synthetic artifact. The latter was implemented as the formula below:

$$a(t) = A_1\exp(-t/\tau_1) + A_2\exp(-t/\tau_2)\cos(2\pi f_0 t+\varphi_0),\ t>0$$

where the constants A_1, A_2, τ_1, τ_2, f_0 and φ_0 are reported in Table I for the two synthetic artifacts shown in Figs.2 and 3 as an example.

In both the cases the synthetic artifact shapes are pretty close to that of the real one, but the "blue" artifact was selected to perform the following computations.

Then the linearly combination of signal s with signal a (s+a) drives the filter in the (7,14) Hz band. If the signal s+a has been previously processed by the algorithm for the electrode-pop artifact detection and removal, the filter output is y_2, otherwise y_1 is obtained. The above mentioned signal x is the filter output when the raw signal s drives the filter. The energy of the two errors e_1 and e_2, and the correspondent SDR_1 and SDR_2 were computed on the limited time intervals of 256 samples and compared to assess the advantage of the application of the new algorithm. Fig.6 shows indeed the energy of the two different errors computed within the above defined windows shifting by 8 samples at time.

The correspondent SDRs behaviors are displayed in Fig.7 where the ratio between the signal energy M_x and the error (either e_1 or e_2) energy M_e is computed over the same 256 samples time interval. Fluctuations of the SDRs curves are due to those of the original EEG signal. From Fig.6 and the next Fig.7 the advantage to apply the algorithm to remove the electrode-pop artifact becomes definitely clear.

In fact, from Fig.7 it can be noted that SDR_2 is constantly 30 dB larger than SDR_1 and is suddenly higher than 0 dB after the artefactual interval where the signal was reset and its values discarded from the following MRD analysis. Indeed, it has to be incidentally mentioned again that the part of the EEG trace between the magenta edges is not taken into account for the following analysis of the MRD and, since the signal in the same interval was canceled, the correspondent SDRs values

are unreliable. After proving the quantitative advantage of the proposed procedure, the algorithm will soon be tested in a real BCI application.

TABLE I. PARAMETERS OF SYNTHETIC ELECTRODE-POP ARTIFACT.

	A_1 [μV]	A_2 [μV]	τ_1 [s]	τ_2 [s]	f_0 [Hz]	φ_0 [rad]
Blue artifact	-1866	350	-0.3	-4	0.10352	0.55287
Green artifact	-1866	350	-0.2	-4	0.10352	0.55287

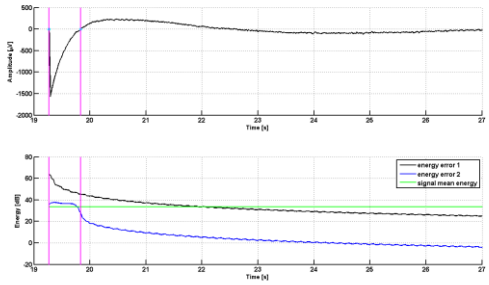

Fig. 6 Energy of the errors at the filter output along with the mean energy level of the original artifact-free signal x (green line) and the artefactual interval (magenta lines).

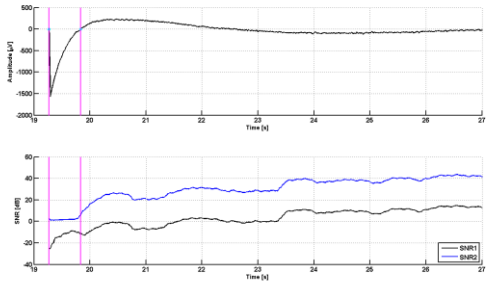

Fig. 7 SDRs at the filter output with the artefactual interval (magenta lines).

It has to be recalled that the BCI platform taken into consideration was described in [10] and its aim was to improve the reaching movement accuracy in mild-impaired post-stroke chronic patients by means of a force feedback that acts as a *mirror* of the cerebral activity related to that action: roughly speaking, while the patient is performing a reaching task on a plane, a force feedback helps him/her in completing the movement only if the expected neural pattern, i.e. spatial and frequency features, is activated. In particular, the MRD is computed in real-time by the BCI2000 software as the normalization of the spectral power around 10 Hz estimated at the current time instant on mean and standard deviation of the analogous quantity gathered during the initial relaxation period. Moreover, these computations are performed on the basis of the recordings coming from specific locations, i.e. the sensorimotor cortex, on the subject's scalp.

If an electrode-pop occurs, all these estimations become affected by abnormal values obtained by filtering the huge impulse present in the signal due to the temporary electrode displacement. Figs.8 to 10 shows the mean energy values obtained during the initial relaxation period, the movement and the correspondent MRD estimation. It has to be recalled from [10] that the more negative the values of the MRD, the more efficient the BCI training. Specifically, Fig.8 is plotted by analyzing the artifact-free dataset where x represents the signal coming from the FZ location.

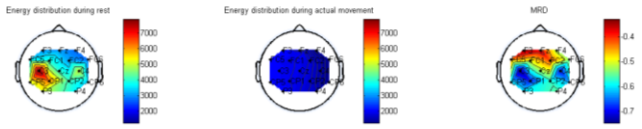

Fig. 8 MRD topography of an artifact-free EEG recording.

Then, Fig.9 shows the disastrous effect of an electrode-pop artifact occurred in the FZ sensor during the initial rest period. The MRD values of this artefactual signal were computed based on y_1.

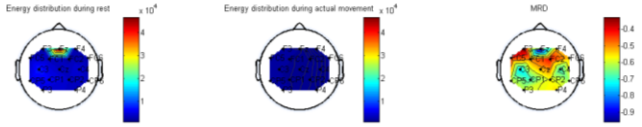

Fig. 9 MRD topography of an artifact-addicted EEG dataset with a synthetic electrode-pop artifact on the FZ site.

As clearly visible from Fig.9, an artefactually huge energy value is focused at the FZ location in the scalp frontal area. While energy distribution during the movement periods of all the following trials is almost within the range of normality, it can be easily expected that the normalization process based on the rest period will lead to unreliable estimation of the patient's cerebral activity, i.e. the MRD values, with a consequent feedback production not related to the physiological activity of the subject and thus useless for him/her motor training.

Finally, Fig.10 reports the analogous energies distributions and MRD estimations gathered after the application of the proposed algorithm that removes the artefactual peak and correctly filters the remaining slow and large overshooting oscillation. Therefore the MRD value of the FZ termination was computed based on y_2. The figure assesses, then, the benefit of such preliminary procedure to remove this kind of artifacts. Indeed, a focus of the activity in C3, Cp1 and C4 is a reasonable expectation since those sites are locations above the sensorimotor cortex: in fact, they belong to the cerebral area where the sensory and motor information is received from the external world, processed and transmitted again to the muscles, the final movement actuators. Moreover, energy values of the rest period are significantly lower than those of the previous case (Fig.9) when the electrode-pop artifact destroyed the EEG physiological waveforms.

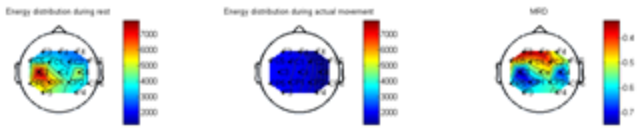

Fig. 10 MRD topography after removing the synthetic electrode-pop artifact from the same EEG dataset of Fig. 8.

DISCUSSION

The previous results assessed the necessity and the effectiveness of the algorithm proposed by the authors to detect and remove the electrode-pop artifact in real-time. From the topographical distribution of the MRD values displayed in Figs.8 to 10 it can be noted that a huge artifact like an electrode-pop occurred in one location of the scalp can compromise the MRD identification and, in particular, increase the number of false positive or false negative detections. Moreover, the effectiveness of the algorithm is also based on its real-time application: in fact, a simple difference operation between consequent amplitude samples (the first derivative step) and the check of its large decrease in few samples (less than 10, i.e. 20 milliseconds) allow the detection of the artifact due to an electrode pop. Furthermore this online identification comes at a very good performance since, as shown in Fig.7, the SDR_2 is constantly much better than the procedure that excludes this detection (SDR_1 curve). As expected, a constant increase of the SDR can be observed as far as the impact of the artifact on the informative signal decreases. As seen from Figs.6 and 7: the first part of the artefactual interval has to be excluded from the following analysis of the MRD because of its artifact abrupt negative slope. An additional interval of time where signal values have to be discarded can be roughly estimated in 1/B, where B is the filter bandwidth (B = 7 Hz in this particular case, then 1/B = 150 ms). In this prolonged period of time - lasting at most one second - the SDRs values are unacceptable (SDR_1) because of the artifact presence or unreliable (SDR_2) because of the signal cancellation in that period. But the most interesting note is that the proposed algorithm suddenly regains a good SDR into respect to the procedure without the artifact detection. As clearly visible from Fig.6, the error energy of the signal preprocessed with the electrode-pop algorithm becomes smaller than the mean energy of the signal immediately after the above defined interval, allowing a much early MRD identification. Concluding, it has to be one more time remarked that the proposed procedure removes only one second of the signal content from the analysis which is a fairly trade-off to have an artifact-free signal, while the current procedure should discard much longer time to wait for the SDR_1 to reach 20 dB (that is the minimum value to have the error energy less than 1% of the useful signal energy, a satisfactory threshold for the MRD evaluations). Finally, it can be observed that if an artifact occurs during the initial long rest period (40 seconds long), both the standard procedure and the new one can correctly estimate the MRD value from the artifact-free remaining part of the rest recording. On the contrary, if it happens during a movement trial (lasting at most one second) it disastrously impacts and the current procedure can not estimate the MRD along several trials, while the new algorithm allows this operation just one second later, that is losing at most one trial (where the BCI feedback would be not provided).

CONCLUSION

In the context of the BCI platform described in [10] an algorithm to detect and remove in real-time rare but huge electrode-pop artifacts was implemented and tested. In particular the shape of this kind of artifacts was mathematically proposed and the performance of the algorithm shown in terms of SDR computed at the band-pass filter output that estimates the signal energy content in the (7,14) Hz band, the typical cerebral rhythms associated with a movement, its planning, observation or even imagination. The energy of the error at the filter output was also computed and this outcome further proves the reliability and efficiency of the algorithm: while the current online BCI procedure provides non-physiology-related and, as a consequence, useless feed-backs to the stroke patient performing the rehabilitative exercise, the presented procedure allows to exploit the EEG data as early as one second after the electrode pop up event. This therefore confirms the convenience of the application of the new algorithm during the online BCI operations since it ensures a more reliable BCI feedback to the patient operating the system.

REFERENCES

[1] E. Niedermeyer, F.H. Lopes da Silva (eds.) *Electroencephalography: basic principles, clinical applications and related fields*, 4th edition, pp. 958–967. Williams and Wilkins, Baltimore, MD, 1999.

[2] N. Birbaumer and L.G. Cohen, “Brain-computer interfaces: communication and restoration of movement paralysis”, *J Physiol*, vol.579, pp.621-636, 2007.

[3] J. S. Barlow, “Automatic elimination of electrode-pop artifacts in EEG's”, *IEEE Trans Biomed Eng*, vol. BME-33, pp.517-521, 1986.

[4] T.P. Jung, S. Makeig, M. Westerfield, J. Townsend, E. Conchesne, T.S. Sejnowski, “Removal of eye activity artifacts from visual event-related potentials in normal and clinical subjects”, *Clin Neurophysiol.*, vol.111, pp. 1745-1758, 2000

[5] P. J. Durka, H. Klekowicz, K. J. Blinowska, W. Szelenberger and S. Z. Niemcewicz, “A simple system for detection of EEG artifacts in polysomnographic recordings”, *IEEE Trans Biomed Eng*, vol. 50, pp. 526-528, 2003.

[6] A. Delorme, S. Makeig, “EEGLAB: an open source toolbox for analysis of single-trial EEG dynamics including independent component analysis”, *J. Neuroscience Methods*, vol. 134, pp. 9-21, 2004

[7] A. delorme, T.J. Sejnowski, S. Makeig, “Enhanced detection of artifacts in EEG data using higher-order statistics and independent component analysis, *Neuroimage,* vol. 34, pp. 1443-1449, 2007

[8] H. Nolan, R. Whelan, R.B. Reilly, “FASTER: Fully automated thresholding for EEG artifact rejection”, *J. Neuroscience Methods*, vol. 192, pp. 152-162, 2010

[9] W.O. Tatum, B.A. Dworetzky, D.L. Schomer, “Artifact and recording concepts in EEG”, J. *Clin Neurophysiology*, vol.28, pp. 252-263, 2011

[10] G. Cisotto, S. Silvoni, M. Cavinato, M. Agostini, F. Piccione and S. Pupolin, “Brain-Computer interface in chronic stroke: an application of sensorimotor closed-loop and contingent force feedback”, , *Proc of IC-C'13*, Budapest, Hungary, pp.2972-2976, 2013.

[11] G. Schalk, D.J. McFarland, T. Hinterberger, N. Birbaumer and J.R. Wolpaw, “BCI2000: A general-purpose brain-computer interface (BCI) system”, *IEEE Trans Biomed Eng*, vol. 51, pp. 1034-43, 2004.

[12] G.Pfurtscheller and F.H.Lopes Da Silva, “Event-related EEG/MEG synchronization and desynchronization: basic principles.”, *Clin. Neurophysiol*., vol.110, pp.1842-1857, 1999.